Ultrawideband Absorbing Boundary Condition for Termination of Waveguiding Structures in FD-TD Simulations

Christopher E. Reuter, *Member, IEEE,* Rose M. Joseph, *Member, IEEE,* Eric T. Thiele, Daniel S. Katz, *Member, IEEE,* and Allen Taflove, *Fellow, IEEE*

***Abstract*— A new method for ultrawideband termination of waveguides in finite-difference time-domain (FD-TD) grids is presented. The Berenger perfectly matched layer (PML) absorbing boundary condition is applied to terminate both perfect electrically conducting (PEC) and dielectric waveguides in two dimensions. Reflections of less than −75 dB are obtained over the entire propagation regime. Evidence is presented that the PML ABC is effective even for the evanescent energy present below cutoff in PEC waveguides and the multimode propagation present in dielectric waveguides.**

I. Introduction

The finite-difference time-domain (FD-TD) method is increasingly being used to model the electromagnetic behavior of not only open-region scattering problems, but also propagation of waves in microwave and optical circuits. An outstanding problem here is the accurate termination of guided-wave structures extending beyond the FD-TD grid boundaries. The key difficulty is that the propagation in a waveguide can be multimodal and dispersive, and the absorbing boundary condition (ABC) utilized to terminate the waveguide must be able to absorb energy having widely varying transverse distributions and group velocities, v_g.

Typical FD-TD ABC's developed for free-space problems include one-way wave equations [1], error-cancelling super-absorbers [2], outgoing wave annihilators [3], and the Liao theory [4]. When applied to terminate dispersive guided wave structures, such ABC's perform best for narrowband energy propagation where v_g is well defined. Recently, these ABC's have been specialized to account for variations of the waveguide modal v_g with frequency. For example, [5] reported the use of a composite ABC operator consisting of N multiplicative first-order linear differential terms. This operator annihilates a propagating pulsed mode at all points along a transverse plane of the waveguide at a set of N desired frequencies, $\{f_i\}$, within the pulse spectrum, corresponding to a set of N analytically calculable group velocities, $\{v_g(f_i)\}$. The number of frequencies at which the annihilation is exact, and thus the bandwidth of the resulting ABC can be increased by adding additional multiplicative terms to the composite operator. A variation of this approach was reported in [6] that approximated the exact $v_g(f)$ with either a linear or a second-order Padé expression. Reference [7] derived a rigorous analytical termination by Laplace transformation of the exact $v_g(f)$. However, this algorithm is global in time, requiring the evaluation of a convolution integral for each mode.

This letter reports a new approach employing a numerical analog of a nonphysical material absorber to yield a robust dispersive ABC for FD-TD simulation of guided-wave systems. This approach is based on the recent Berenger perfectly matched layer (PML) concept [8], [9]. The new approach has the advantages of being local in time and space, general, and extremely accurate over a wide range of group velocities. It requires no knowledge of the modal distribution or dispersive nature of the propagating field.

II. Method

The Berenger PML ABC provides a means to terminate FD-TD grids essentially without reflection using a nonphysical lossy medium adjacent to the outer grid boundary. Within the PML, certain field components are split into subcomponents. This splitting introduces an additional degree of freedom in specifying material parameters that permits waves of arbitrary frequency and angle of propagation to rapidly decay and yet maintain the velocity and field impedance of the lossless dielectric case. The PML can thus be "perfectly matched" to an interior medium for all wave angles and frequencies. For 2-D and 3-D scattering models, [8] and [9] reported local reflections of outgoing cylindrical or spherical waves by PML as low as 1/3000th those of standard ABC's and global error energy in the 2-D FD-TD mesh declining by 10^{12}.

Consider the use of PML to terminate general waveguiding structures for 2-D modes having the field components E_x, E_y, and H_z. Here, the PML formulation specifies four rather than the usual three coupled field equations because H_z is split into two subcomponents, H_{zx} and H_{zy}:

$$\varepsilon_d \frac{\partial E_x}{\partial t} + \sigma_y E_x = \frac{\partial (H_{zx} + H_{zy})}{\partial y} \tag{1a}$$

$$\varepsilon_d \frac{\partial E_y}{\partial t} + \sigma_x E_y = -\frac{\partial (H_{zx} + H_{zy})}{\partial x} \tag{1b}$$

$$\mu_d \frac{\partial H_{zx}}{\partial t} + \sigma_x^* H_{zx} = -\frac{\partial E_y}{\partial x} \tag{2a}$$

Manuscript received June 3, 1994. This work was supported in part by NSF Grant ECS-9218494, ONR Contract N00014-93-0133, NASA-Ames Contract NAS2-13890, and Cray Research, Inc.

C. E. Reuter, R. M. Joseph, E. T. Thiele, and A. Taflove are with the Electrical Engineering and Computer Science Department, McCormick School of Engineering, Northwestern University, Evanston, IL 60208 USA.

D. S. Katz is with Cray Research, Inc., El Segundo, CA 90245 USA.

IEEE Log Number 9405079.

$$\mu_d \frac{\partial H_{zy}}{\partial t} + \sigma_y^* H_{zy} = \frac{\partial E_x}{\partial y} \tag{2b}$$

Electric loss, σ, and magnetic loss, σ^*, can be assigned to the electric and magnetic field components as indicated to cause exponential decay of propagating fields in the PML region. If

$$\frac{\sigma_x}{\varepsilon_d} = \frac{\sigma_x^*}{\mu_d}, \quad \frac{\sigma_y}{\varepsilon_d} = \frac{\sigma_y^*}{\mu_d} \tag{3}$$

is enforced, where ε_d and μ_d are the PML permittivity and permeability, this decay can take place in a frequency-independent manner without impacting the wave impedance [8].

Now, consider as a specific subset of (1) and (2) the case of a 2-D dielectric-filled (ε_d, μ_d) waveguide structure propagating one or more TM modes in the $+x$ direction. At $x_{\max}$, the waveguide is loaded with PML that has σ_x and σ_x^* matched according to (3) along with with $\sigma_y = \sigma_y^* = 0$ to permit reflectionless transmission across the dielectric-PML interface [8]. We assume as in [8] that the loss in the PML region increases quadratically with depth, ρ. That is, the loss rises from zero at $\rho = 0$ (the interface between the waveguide dielectric and the PML load) to a maximum value of $\sigma_{\max}$ at $\rho = \delta$, the location of the conducting wall backing the PML:

$$\sigma(\rho) = \sigma_{\max}\left(\frac{\rho}{\delta}\right)^2 \tag{4}$$

Then, $\sigma_{\max}$ can be chosen to bound the apparent reflection coefficient

$$R = e^{-\frac{2\sigma_{\max}\delta}{3\varepsilon_d c}} \tag{5}$$

to some desired low level, say 10^{-4}. Note that the resulting exponential decay within the PML load is so rapid that the standard Yee time-stepping cannot be used there. Instead, exponential time-stepping [8], [10] is used in PML media with values of ε_d and μ_d employed in the decay factors.

III. Results

We first apply PML to an air-filled 2-D PEC parallel-plate waveguide (Fig. 1(b)) having a wall separation of 40 mm ($f_{\text{cutoff}} = 3.75$ GHz). Excitation consists of an 83.3-ps Gaussian pulse (FWHM) modulating a 7.5-GHz carrier that launches an $+x$-directed TM_1 mode towards the PML termination. The spectrum of the input pulse is shown in Fig. 1(a) along with the normalized v_g for the TM_1 mode. Note that the incident pulse contains significant energy below cutoff, and that v_g of the pulse spectral components ranges from 0 to ≈ 0.98 c. The PML is 16 grid cells thick with σ_x varying quadratically from zero at the air-PML interface to 2.00 S/m at the back PEC wall, and the associated magnetic loss, σ_x^*, varing from zero to 2.85$\times$ 10^5 Ω/m. Before discrete Fourier transformation (DFT), the reflected wave observed at the air-PML interface is allowed to evolve over many thousands of time steps to properly model the action of the very slowly propagating fields having spectral components near f_{cutoff}, which results in a very slowly decaying impulse response for the PML termination. The reflection coefficient versus frequency is obtained by dividing the reflected spectrum by the incident spectrum as observed at the air-PML interface.

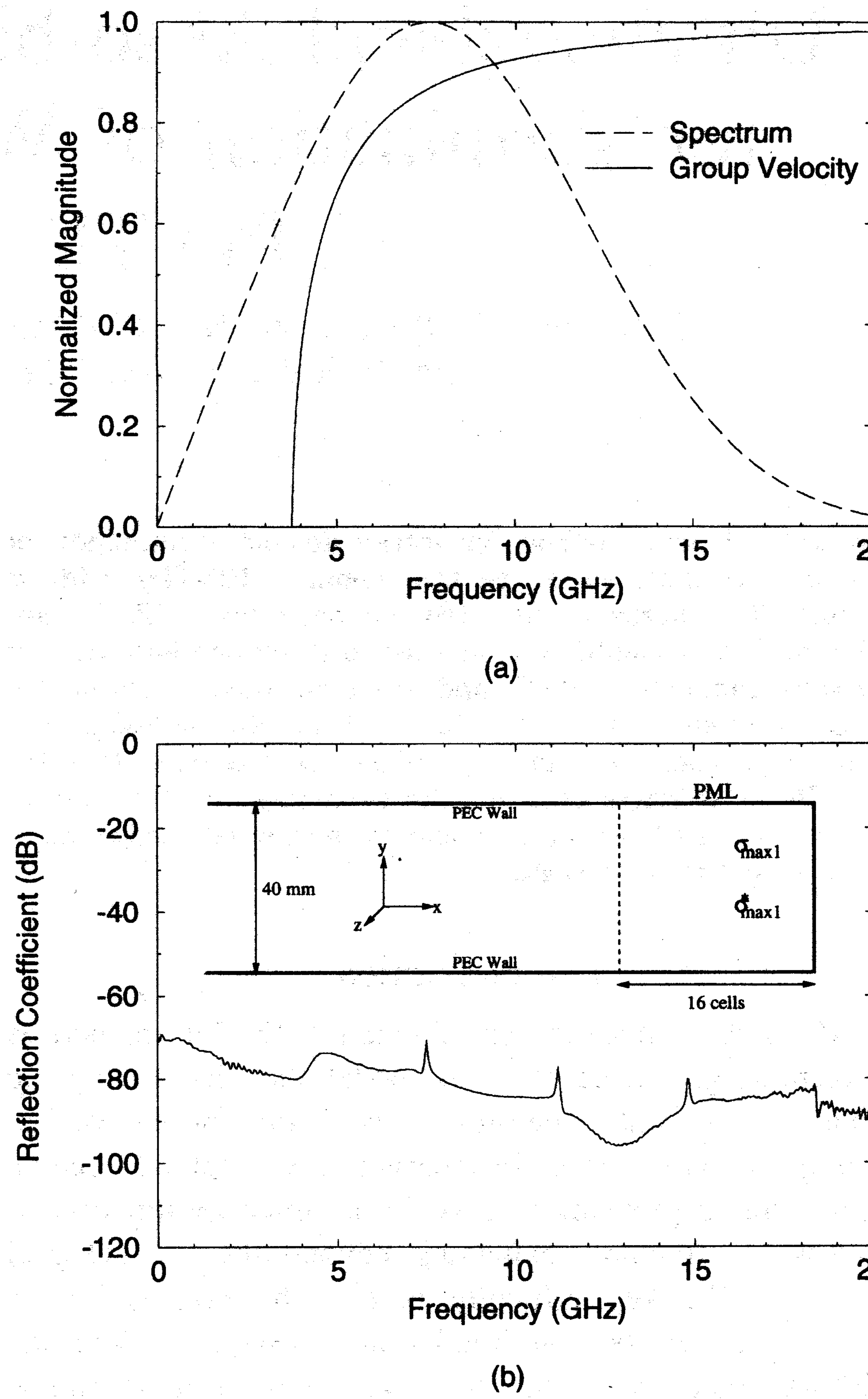

Fig. 1. Test of PML ABC for a 2-D PEC microwave waveguide propagating a pulsed TM_1 mode: (a) Excitation spectrum superimposed upon the group velocity versus frequency function for the TM_1 mode (cutoff frequency = 3.75 GHz). (b) Waveguide/PMLgeometry and PML reflection coefficient versus frequency observed just outside the PML layer.

Fig. 1(b) graphs the reflection coefficient of the PML ABC versus frequency. Reflections between -70 and -95 dB are noted at *all* frequency points in the DFT from the lowest ($\approx f_{\text{cutoff}}/100$) to the higest ($\approx 5.3 f_{\text{cutoff}}$). Narrow 8-dB upwards spikes are noted at $f = 2f_{\text{cutoff}}$, $3f_{\text{cutoff}}$, and $4f_{\text{cutoff}}$. This example vividly demonstrates the ability of the PML ABC to absorb extremely wideband propagating energy as well as highly reactive evanescent modes.

We next apply the PML ABC to terminate a 2-D asymmetric dielectric slab optical waveguide (Fig. 2(b)). This consists of a 1.5-μ film of $\varepsilon_r = 10.63$ sandwiched between an infinite substrate of $\varepsilon_r = 9.61$ and an infinite region of air. A 17-fs (FWHM) Gaussian pulse modulating a 200-THz carrier at the left edge of the three-layer system launches three distinct $+x$-directed modes with normalized frequency-dependent propagation factors shown in Fig. 2(a). The system is terminated by extending each dielectric layer into its matching PML region at the right side of the grid. The PML is

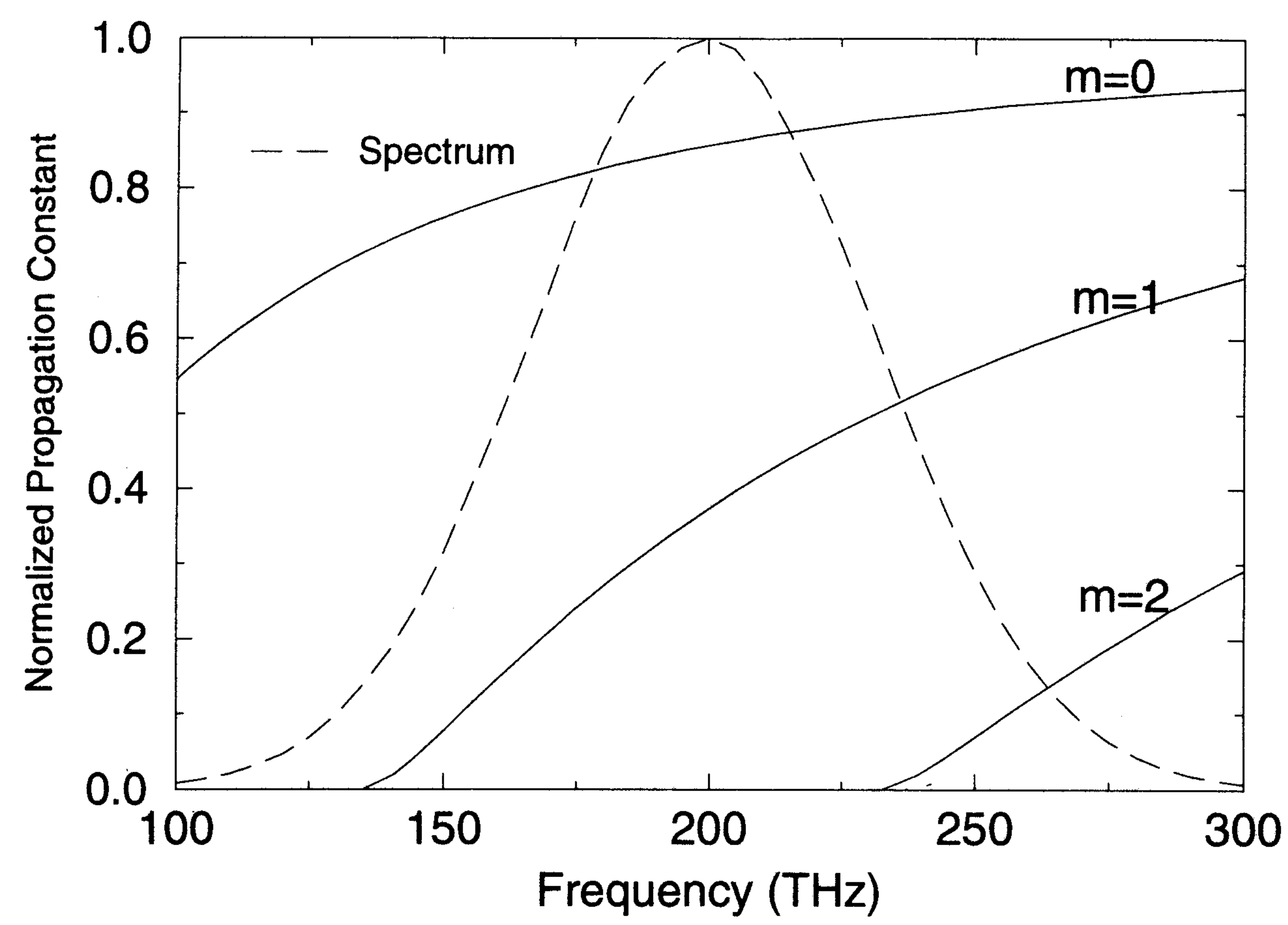

(a)

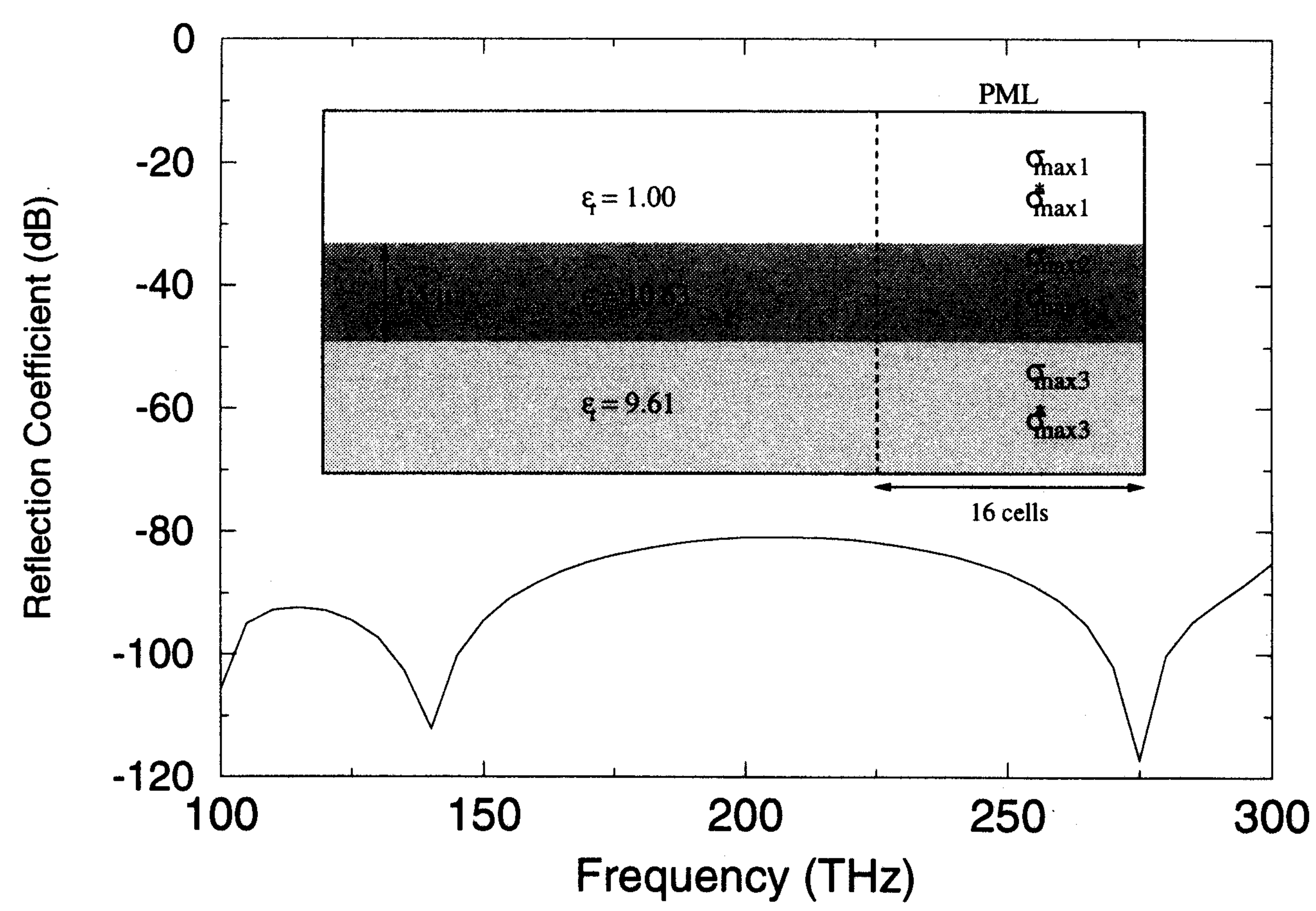

(b)

Fig. 2. Test of PML ABC for a 2-D asymmetric three-layer dielectric optical waveguide propagating three distinct modes: (a) Excitation spectrum superimposed upon the propagation factors for the three modes. (b) Waveguide/PML geometry and PML reflection coefficient versus frequency observed just outside the PML layer. Note that the substrate and air regions extend to infinity in the transverse direction, and that optical wave energy is present in all three regions.

again 16 cells thick with (σ_x, σ_x^*) varying quadratically in the x-direction from 0 at each layer-PML interface to peak values of (1.39×10^5 S/m, 1.98×10^{10} Ω/m) in the air region, (1.48×10^6 S/m, 1.98×10^{10} Ω/m) in the film, and (1.34×10^6 S/m, 1.98×10^{10} Ω/m) in the substrate. The composite reflection coefficient representing total retrodirected energy in all three regions is computed at the PML interface. Fig. 2(b) shows reflections below -80 dB across the entire spectrum of the incident field. This demonstrates the absorptive capability of the PML ABC for dispersive multimodal propagation. In this case, as well, the PML ABC absorbs the evanescent portion of the propagating modes as well as any radiated energy.

IV. Conclusion

We have demonstrated the use of the Berenger PML ABC for highly accurate ultrawideband termination of 2-D PEC and dielectric waveguides in FD-TD grids. This ABC is local in time and space and yields broadband reflection coefficients better than -75 dB. It appears to be effective for absorption of dispersive, multimodal, and even evanescent energy. Extension of PML to 3-D PEC and dielectric waveguides is straightforward and will be discussed in a subsequent paper. Another potentially useful application is for the FD-TD modeling of problems involving the earth-air interface, a subset, in fact, of the three-layer dielectric geometry discussed here.

References

[1] G. Mur, "Absorbing boundary conditions for the finite-difference approximation of the time-domain electromagnetic field equations," *IEEE Trans. Electromagn. Compat.*, vol. EMC-23, pp. 377–382, Nov. 1981.

[2] K. K. Mei and J. Fang, "Superabsorption—a method to improve absorbing boundary conditions," *IEEE Trans. Antennas Propagat.*, vol. AP-40, pp. 1001–1010, Sept. 1992.

[3] A. Bayliss and E. Turkel, "Radiation boundary conditions for wave-like equations," *Commun. Pure Appl. Math.*, vol. 33, pp. 707–725, 1980.

[4] Z. P. Liao, H. L. Wong, B. P. Yang, and Y. F. Yuan, "A transmitting boundary for transient wave analysis," *Scientia Sinica* (series A), pp. 1063–1076, Oct. 1984.

[5] Z.-Q. Bi, K.-L. Wu, C. Wu, and J. Litva, "A dispersive boundary condition for microstrip component analysis using the FD-TD method," *IEEE Trans. Microwave Theory Tech.*, vol. MTT-40, pp. 774–777, Apr. 1992.

[6] J. C. Olivier and D. A. McNamara, "Analysis of multiport discontinuities in waveguide using a pulsed FD-TD approach," *IEEE Trans. Microwave Theory Tech.*, in press.

[7] F. Moglie, T. Rozzi, P. Marcozzi, and A. Schiavoni, "A new termination condition for the application of FD-TD techniques to discontinuity problems in close homogeneous waveguide," *IEEE Microwave and Guided Wave Lett.*, vol. 2, pp. 475–477, Dec. 1992.

[8] J.-P. Berenger, "A perfectly matched layer for the absorption of electromagnetic waves," *J. Computational Physics*, in press.

[9] D. S. Katz, E. T. Thiele, and A. Taflove, "Validation and extension to three dimensions of the Berenger PML absorbing boundary condition for FD-TD meshes," *IEEE Microwave and Guided Wave Lett.*, vol. 4, no. 3, pp. 268–270, Aug. 1994.

[10] R. Holland, "Finite-difference time-domain (FD-TD) analysis of magnetic diffusion," *IEEE Trans. Electromagn. Compat.*, vol. 36, pp. 32–39, Feb. 1994.